Hydrogels That Actuate Selectively in Response to Organophosphates

*Manos Gkikas, Reginald K. Avery, Carolyn E. Mills, Ramanathan Nagarajan, Eugene Wilusz, and Bradley D. Olsen**

Nerve agents and pesticides represent a category of extremely toxic organophosphate compounds (OPs) that irreversibly inhibit the enzyme acetylcholinesterase, disturbing transmission in the synaptic clefts of muscles and nerves. Protection from these compounds necessitates the development of breathable barriers that can selectively block the passage of OPs. Hydrogels prepared from acrylamide, N,N′-methylene*bis*(acrylamide), N,N′-*bis*(acryloyl) cystamine, and hydrophilic pendant oximes are herein prepared, showing the ability to decontaminate and respond to the presence of OPs through a change in swelling. The oxime-based hydrogels show selective response only to malaoxon when tested against chemicals that are found in sweat as well as other reactive chemicals that are found in the environment. Pore sealing is demonstrated in perforated equilibrated gels within 3–4 h after the addition of malaoxon, showing actuation of the gel in response to organophosphates. This strategy demonstrates the ability to couple oxime-based decontamination and disulfide chemistry to produce hydrogels that can decontaminate organophosphate compounds, sense the decontamination product, and transduce this sensing response into actuation of the gel, which can be used to close pores in gel sheets or between fibers in a protective fabric coating.

1. Introduction

Organophosphate compounds (OPs) are widely used as pesticides and chemical warfare agents (such as the nerve agents soman, sarin, and venomous agent X,VX); these toxic chemicals lead to neuromuscular paralysis[1] due to the irreversible phosphorylation of acetylcholinesterase (AChE).[2–8] Among the OP compounds, the V-type nerve agents are the most toxic, rendering the development of novel decontamination and protection technologies highly important. Decontamination or sequestration of high toxicity OP compounds can be accomplished through hydrolysis of the phosphate ester bond[9–12] with the enzyme organophosphorus hydrolase,[9–15] entrapment in nanoporous materials,[16,17] enzyme/polymer conjugates[18–24] and highly bioactive enzyme/amphiphilic polymer formulations,[25] chemically modified fluorescent probes,[26–28] and oxime reactivators.[29–32] V-type organophosphates contain a P–S bond and a choline-like moiety and are hydrolyzed very slowly by natural enzymes. Therefore, new and efficient approaches that target VX are necessary for mitigation of the agent.

A major challenge in the mitigation of threats from OP compounds is developing protective garments that can eliminate exposure of the wearer to the toxic chemical. Some rubbers can serve as effective barrier materials,[33] but in sufficient thickness they are not breathable and extremely uncomfortable to wear for an extended period of time. Therefore, there is a strong interest in a garment or barrier membrane that could remain in a porous state when it is not in the presence of an organophosphate, but close its pores autonomously in the presence of the toxic agent to prevent its passage. Such a smart barrier needs to be able to efficiently sense the OP compound and also transduce the sensing response into an actuated change of state without an external input of energy.

The reactivity of oximes with OP compounds, yielding phosphorylated adducts,[34–44] provides a potential basis for detection and response in an autonomous material. As part of antidotal therapy against OP poisoning, oximes help reactivate phosphorylated AChE. Quaternary pyridine aldoximes substituted in the para position have been shown to be highly reactive in reversing poisoning from different OP compounds, screened over AChE of different origins.[36] Polymeric materials with enhanced nucleophilic activity provided by N-alkyl 4-pyridinium aldoximes also recently showed significant detoxification of diisopropyl fluorophosphate.[31]

Coupling oxime decontamination with responsive crosslinkers could potentially enable the triggering of responsive

Dr. M. Gkikas, C. E. Mills, Prof. B. D. Olsen
Department of Chemical Engineering
Massachusetts Institute of Technology
Cambridge, MA 02139, USA
E-mail: bdolsen@mit.edu
Dr. M. Gkikas, Prof. B. D. Olsen
Institute for Soldier Nanotechnologies
Cambridge, MA 02139, USA
R. K. Avery
Department of Biological Engineering
Massachusetts Institute of Technology
Cambridge, MA 02139, USA
Dr. R. Nagarajan, Dr. E. Wilusz
Natick Soldier Research
Development & Engineering Center
Natick, MA 01760, USA

DOI: 10.1002/adfm.201602784

hydrogels, taking advantage of the decomposition products released by nerve agents after reaction with oximes and the subsequent reaction with cross-linkers. Such a design would allow the sensing and decontamination of OPs through reaction with oximes and induced volumetric changes within the gel. Many types of hydrogels have been engineered as building blocks for different stimuli-responsive materials due to their biocompatibility, biodegradability, tunability in mechanical properties, and molecular recognition abilities.[45–48] Recently, N,N-bis(acryloyl cystamine) (BAC) was used as the bridging molecule in radical polymerization, enabling numerous applications that are triggered by external stimuli such as pH, temperature, ionic strength, light, stress, and ligand binding (ligand-triggered actuators/sensors) to modulate the state of the disulfide bond.[49–53]

Herein, the ability to couple oxime-based decontamination and disulfide chemistry is demonstrated, producing hydrogels that can decontaminate organophosphate compounds, sense the decontamination product, and transduce this sensing response into actuation of the gel which could be used to close pores in a gel layer or on a fabric coating. Hydrogels containing acrylamide (AAM), BAC, N,N′-methylene*bis*(acrylamide) (Bis), and an oligo(ethylene glycol)-acrylate monomer of pyridine-4-aldoxime (acryl-EG_5-oxime) were prepared from cheap, commercially available materials, using free radical polymerization at room temperature (RT), and were screened against the organophosphorous compound malaoxon, a simulant for the chemical warfare agent VX. The reaction of oximes with malaoxon or any other thiol-containing organophosphate (such as demeton, demeton S, and disulfoton) liberates thiolate ions, and these thiols cleave a fraction of the chemical cross-links in the gels, which are formed by disulfide bridges. This can simultaneously swell the gel and decontaminate the agent, while the swelling response is transduced into a mechanical response within the material. Gel response to malaoxon was examined over time, and several gel constructs were fabricated to demonstrate the ability to generate mechanical actuation. The oxime-based hydrogel was applied as a coating on fibers, leading to a swellable protective layer that can potentially seal pores in the fabric.

2. Results and Discussion

2.1. Oxime Decontamination and Synthesis of Responsive Hydrogels

The reaction of oxime with malaoxon rapidly degrades the organophosphate, producing a thiolate ion as a byproduct. This reaction scheme is general to all the V-type organophosphates, containing a thiol leaving group with a choline-like moiety, including the nerve agent VX. The thiol byproduct may then be used as an analyte for colorimetric detection or as a chemical trigger for a responsive hydrogel based on disulfide exchange reactions. To quantify the kinetics of the reaction, the commercially available water-soluble oxime, pyridine-2-aldoxime methochloride (100×10^{-3} M), was reacted with malaoxon (0.1×10^{-3} M) in the presence of Ellman's reagent, DTNB: 5,5′-dithiobis(2-nitrobenzoic acid) (1.0×10^{-3} M).[54]

The decontamination reaction showed a fast time-dependent response, seen as a colorimetric change (**Figure 1**). Since the reaction between oxime and malaoxon liberates thiolate ions, the Ellman's reagent was used as a colorimetric scavenger due to the strong absorbance of the liberated 2-nitro-5-thiobenzoate anion (TNB^{2-}) at 412 nm[54] (Figure S1, Supporting Information). As a negative control, reaction of oxime with only DTNB showed no colorimetric response (Figure 1a). Kinetics measurements at 412 nm showed an exponential response to malaoxon over time (Figure 1b). By fitting the data to Equation (1), apparent rate constants k_1 and k_2 were calculated. Concentration dependence of the apparent rate constants showed a linear response (Figure 1c), which led to estimation of the rate constants, $k_{ox.} = 0.0711 \pm 0.0001$ $M^{-1} \times min^{-1}$ and $k_{s.} = 317.2 \pm 18.4$ $M^{-1} \times min^{-1}$. These results establish kinetic parameters for estimating the response rate in oxime-functionalized hydrogels.

The incorporation of oxime-functionalized monomers and cleavable disulfide cross-links in polymer hydrogels allows for the dissolution (BAC only) or the swelling of gels (BAC

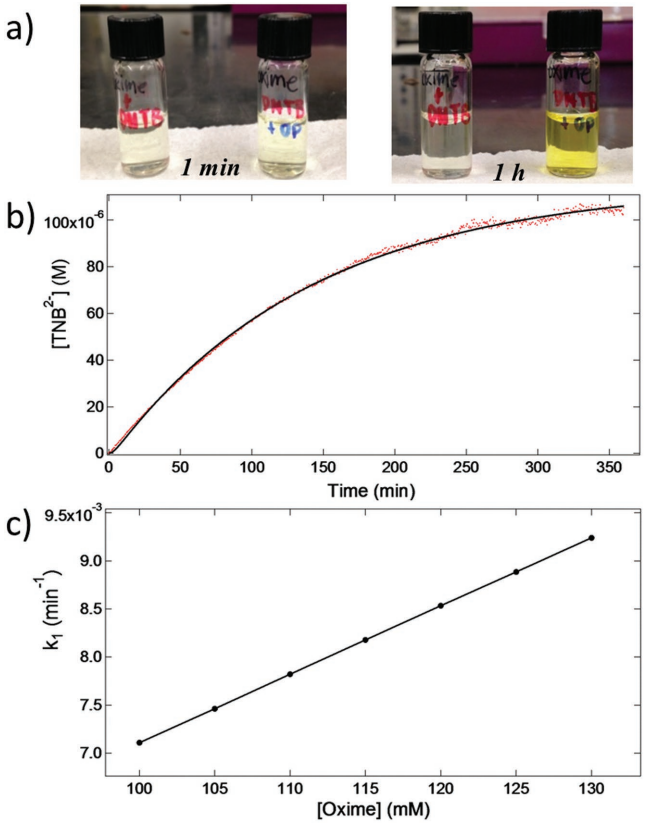

Figure 1. a) Photos of vials containing the water soluble pyridine-2-aldoxime methochloride with DTNB (on the left) as well as after malaoxon addition (on the right), after 1 min and 1 h. Oximes react with malaoxon, liberating thiolate ions that are able to cleave the Ellman's reagent (DNTB), yielding benzyl-thiolate ions (TNB^{2-}, yellow color). DNTB itself does not react with the oxime. b) Kinetics of the reaction fitted to Equation (1), leading to estimates of the apparent rate constants. c) Observed rate constants (k_1) as a function of the concentration of oxime, indicating that the reaction is first order in oxime. The slope provides the oxime rate constant ($k_{ox.}$).

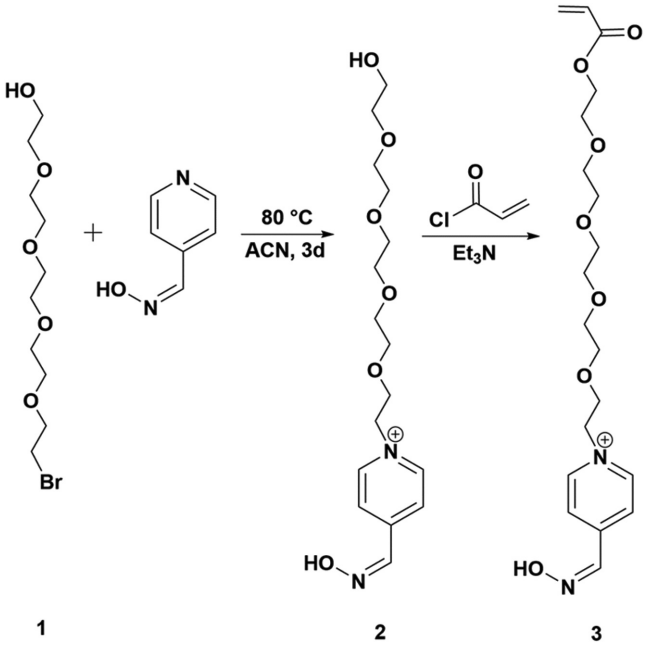

Scheme 1. Chemical reactions to obtain the hydrophilic pendant acryl-EG_5-oxime from commercially available materials.

and Bis) to be modulated based on the same degradation and disulfide exchange mechanism. To prepare oxime functional gels, pyridine-4-aldoxime was reacted with bromo-EG_5-alcohol (1) leading to a quaternized oxime, bearing a hydrophilic oligo(ethylene glycol) chain (2). Subsequent reaction with acryloyl chloride led to the acryl-EG_5-oxime (3), as is shown in **Scheme 1** (compound characterization in Figures S2–S6, Supporting Information). Two types of gels were prepared, based on utilization of only BAC as the bridging molecule (9 wt% AAM), or both Bis and BAC (8 wt% AAM). Combination of 9 wt% AAM with BAC and acryl-EG_5-oxime led to the formation of transparent yellow AAM/BAC/oxime hydrogels within 10 min, in comparison with the transparent AAM/BAC gels having no oxime. AAM/Bis/BAC/oxime hydrogels were also prepared at 2:1 Bis/BAC molar ratio, using 8 wt% AAM, BAC, and Bis as an additional cross-linking monomer. The gelation occurred within 1–2 min, much faster than the gelation using only BAC due to the higher overall cross-linker concentration. The polymerized gels were cloudy yellow, in comparison with the cloudy AAM/Bis/BAC gels having no oxime (**Figure 2**). The opacity of Bis/BAC gels denotes inhomogeneity, probably due to the additional cross-linker.

2.2. Agent Degradation and Mechanical Actuation of Hydrogels

Gels containing acryl-EG_5-oxime and disulfide cross-linkers (BAC) rapidly degrade in the presence of malaoxon. The gels were initially swollen to an equilibrium state in water, resulting in a 66% increase in weight after a 3 d equilibration from the initial relaxed state (Figure S7, Supporting Information). After the addition of 73.0×10^{-3} M malaoxon (molar ratio of malaoxon to oxime is 7:1), the hydrogels rapidly degraded, as shown in **Figure 3**, leading to complete dissolution (100%). If the same volume of water was added instead of malaoxon in the equilibrated gels, only a minimal volume change was observed. Gel erosion images over time are shown in Figure 3b. Erosion profiles were also obtained for 36.5 and 18.3×10^{-3} M malaoxon, leading to 86 and 67 wt.% erosion, respectively, for equivalent incubation times. By fitting the data to the Korsmeyer–Peppas equation (Equation (2)), rate constants for gel degradation were obtained (**Table 1**). Increasing malaoxon concentrations resulted in higher degradation rate constants, while the exponent n, which characterizes the mechanism of

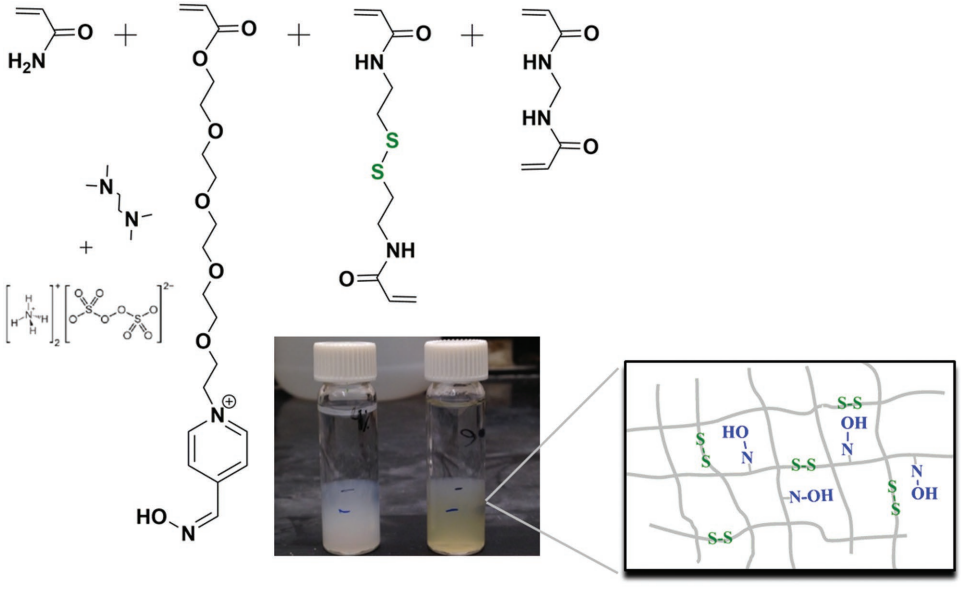

Figure 2. AAM/Bis/BAC/oxime hydrogels obtained from free radical copolymerization at room temperature (RT). The resultant oxime-containing gels are yellow due to the incorporation of the colored oxime monomer in comparison with the AAM/Bis/BAC gels.

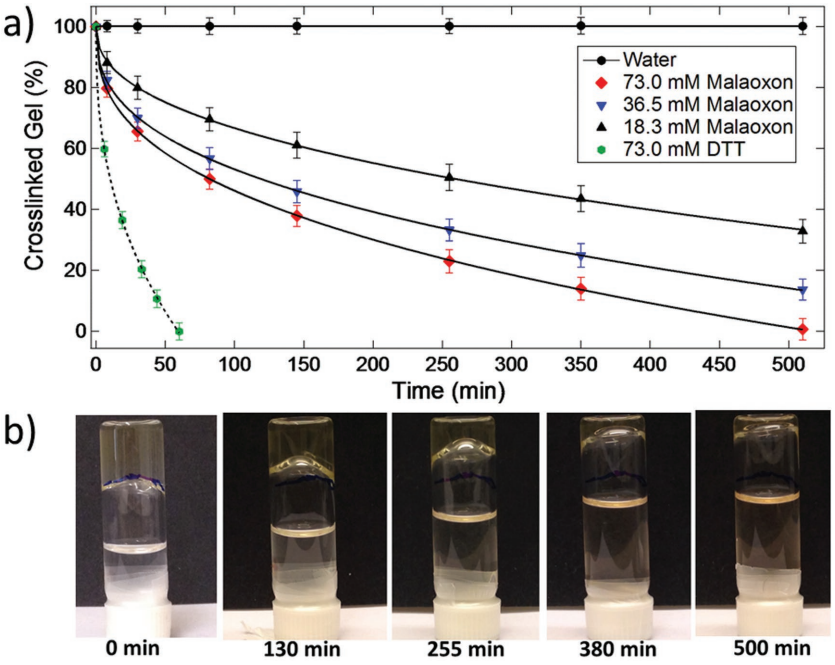

Figure 3. a) Time-dependent response of AAM/BAC/oxime hydrogels against 18.3×10^{-3}, 36.5×10^{-3}, 73.0×10^{-3} M malaoxon, 73.0×10^{-3} M DTT, and water. Solid and dotted lines represent fits to the Korsmeyer–Peppas equation. b) Gel erosion photos of AAM/BAC/oxime hydrogels over time against 73.0×10^{-3} M malaoxon.

release, decreased. The rate constants were estimated to be 9.5 ± 0.1 min^{-n} for 73.0×10^{-3} M malaoxon, 8.3 ± 0.1 min^{-n} for 36.5×10^{-3} M malaoxon, and 4.7 ± 0.1 min^{-n} for 18.3×10^{-3} M malaoxon. The AAM/BAC/oxime gels were also tested against the thiol-containing molecule DL-dithiothreitol (DTT) to show that the degradation is specifically due to the cleavage of the disulfide bonds. Addition of 73.0×10^{-3} M DTT showed a fast response over time with a rate constant of 19.8 ± 0.3 min^{-n} (Figure 3a). The faster rate is potentially due to the direct reaction between the dithiols (DTT) and the disulfide cross-linker.[53,55] In the case of malaoxon, the pendant oximes have to react first with the agent in a slower, rate-determining step ($k_{ox.} = 0.0711$ $M^{-1} \times min^{-1}$) before liberating thiolate ions ($k_s = 317.2$ $M^{-1} \times min^{-1}$). Additionally, the primary thiols of DTT are expected to react faster than the secondary liberating thiols of malaoxon.

When permanent chemical cross-links are incorporated into the gels in addition to disulfide cross-links, the gels swell in response to malaoxon. Gels containing AAM, acryl-EG_5-oxime, Bis, and disulfide cross-linkers (BAC) were pre-equilibrated for 3 d in water (Figure S8, Supporting Information). Addition of 73.0×10^{-3} M malaoxon after this equilibration resulted in swelling up to 9.5% (w/w) (endpoint weight change from equilibrium), showing that the gel can actuate in the presence of the toxic agent (**Figure 4**). To test the sensitivity of the hydrogels, different concentrations of malaoxon were examined. Addition of 36.5×10^{-3} M malaoxon showed a swelling response of 7.3%, while 18.3×10^{-3} M malaoxon showed a swelling response of 3.4% at the same incubation time (Figure 4a). To assess the network structure of oxime gels, the number of effective cross-linked chains per cross-linkable (Bis+BAC) molecule, U_e* (calculated with Equations (3) and (6), respectively) was used to estimate the network structure from swelling data. The value of U_e* gives an estimate of the type of cross-linking occurring in these network structures, with U_e* > 1 suggesting entanglements in the network structure of the material. The number of normalized effective cross-links in the gel decreased from 0.536 (water equilibria) to 0.486, 0.439, and 0.416 after exposure to 18.3×10^{-3}, 36.5×10^{-3}, and 73.0×10^{-3} M malaoxon, respectively (Figure 4c).

2.3. Selectivity of Oxime-Based Hydrogels

The oxime-based hydrogels were also tested against chemicals that are found in sweat and in the environment, showing selective response only to malaoxon (Figure 4d). The extreme scenario of 73.0×10^{-3} M (>1 wt%) of each compound was examined, showing a high degree of selectivity toward organophosphates. Only 73.0×10^{-3} M KOH resulted in slight swelling (0.8% swelling) (Figure 4d). Swelling kinetics of AAM/Bis/BAC/oxime gels were similar for 73.0×10^{-3} M malaoxon and 73.0×10^{-3} M DTT. AAM/Bis/BAC gels were cloudy upon formation, and became transparent after the addition of 73.0×10^{-3} M DTT (Figure 4b), showing a rapid increase in transparency over time as swelling reached ≈10.0% (linear change, Figure S9, Supporting Information). Addition of 36.5×10^{-3} M DTT led to rapid swelling for the first 5 h before reaching a plateau. After 22 h, swelling increased again and reached a final value of 6.3% after 50 h (Figure S9, Supporting Information). Equilibrated oxime gels rapidly swelled to 8.7% with the addition of 73.0×10^{-3} M malaoxon, with a similar kinetic profile to 73.0×10^{-3} M DTT (Figure S9, Supporting Information). Kinetic swelling profiles after the addition of 36.5×10^{-3} and 18.3×10^{-3} M malaoxon were similar, both having an increase in swelling with time that reached a plateau after 22 h, with endpoint swelling values of 3.4 and 5.0%, respectively (Figure S9, Supporting Information).

2.4. Pore Closing and Oxime-Gel Fabric Impregnation

This swelling mechanism can simultaneously sense organophosphates, decontaminate them by reactive degradation, and

Table 1. Kinetic parameters of the eroded gels obtained from the Korsmeyer–Peppas model.

Agent Added	k [min^{-n}]	n
73.0×10^{-3} M malaoxon	9.5 ± 0.1	0.376 ± 0.003
36.5×10^{-3} M malaoxon	8.3 ± 0.1	0.377 ± 0.002
18.3×10^{-3} M malaoxon	4.7 ± 0.1	0.426 ± 0.004
73.0×10^{-3} M DTT	19.8 ± 0.3	0.396 ± 0.004

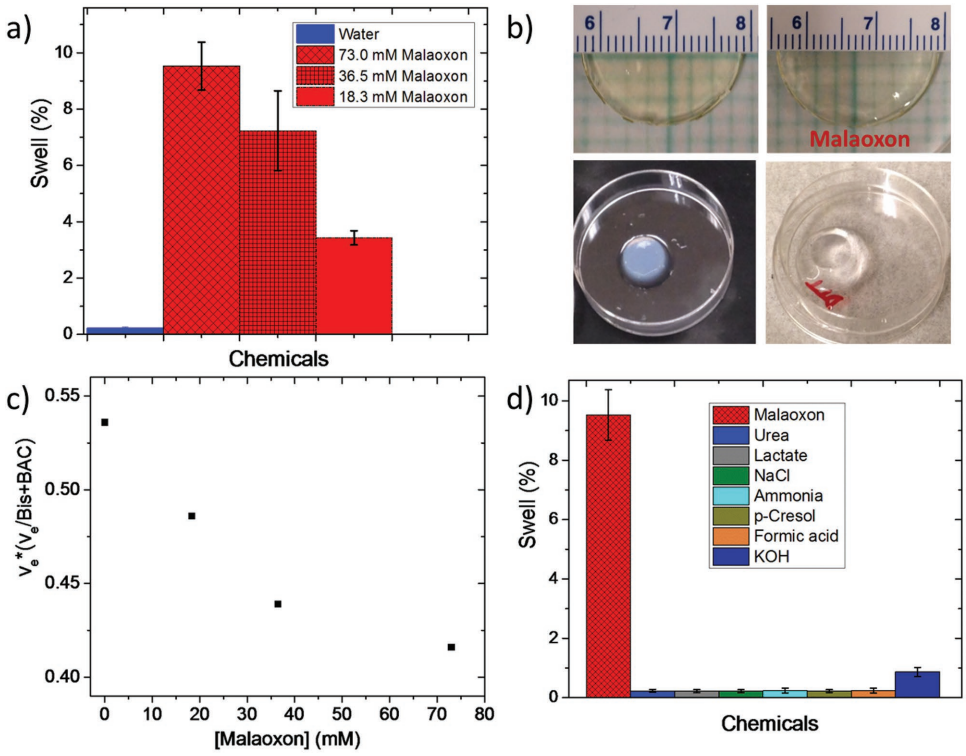

Figure 4. a) Endpoint swelling response of equilibrated AAM/Bis/BAC/oxime gels using 73.0×10^{-3}, 36.5×10^{-3}, and 18.30×10^{-3} M malaoxon. b) Swelling response of equilibrated AAM/Bis/BAC/oxime gels and AAM/Bis/BAC gels before (left) and after (right) addition of 73.0×10^{-3} M of malaoxon and 73.0×10^{-3} M DTT, respectively. The non-oxime gels are cloudy upon formation and become transparent in the presence of DTT. c) Dependence of normalized effective cross-links on malaoxon concentration. d) Swelling response of equilibrated AAM/Bis/BAC/oxime gels using 73.0×10^{-3} M of malaoxon, urea, lactate, sodium chloride, ammonia, *p*-cresol (sweat chemicals), as well as 73.0×10^{-3} M of KOH and formic acid, showing selectivity to organophosphates.

actuate the hydrogel to close pores. When the oxime hydrogels were perforated, pore closing was observed after the addition of malaoxon. Equilibrated gels were punctured with microneedle arrays, and were then imaged with an optical microscope before and after malaoxon addition (**Figure 5**), showing actuation of the gel in response to organophosphates. An equilibrated gel is shown in Figure 4a. The black spot is a void in the gel due to puncturing (Figure 5b). Malaoxon swells the oxime hydrogels, filling the voids, in response to the agent (Figure 5c). It was found that a ≈250 µm hole could be fully filled with swelled material within 3–4 h (video, Supporting Information).

Alternately, the oxime-based gels can be coated onto fibers, where they can also swell selectively in response to organophosphate agents. Water-equilibrated oxime hydrogel-coated fabric responded fast against the toxic agent, yielding a yellow color of increased intensity with time due to the liberation of 2-nitro-5-thiobenzoate anions (DTNB was used as a free thiol scavenger). The fabric-coated oximes react with malaoxon, releasing thiolate ions that were detected as by-products (Figure 5d,e). In this way, the oxime-hydrogel fabric protects effectively against organophosphate compounds. It is important to note that prior to the addition of the agent, the oxime-gel coated-fabric was equilibrated for 3 d by water exchange, so as to remove any free oximes. Silk coated with the oxime-based gel showed a mechanical response in the presence of malaoxon (Figure 5f–i). Neat silk shows autofluorescence between 310–465 nm (4′,6-diamidino-2-phenylindole (DAPI) filter: Exc. 358 nm/Em. 461 nm),[56] while the pores of hydrated silk were clearly visible (Figure 5f). Polymerizing acryl-treated silk with a 30 wt% AAM/Bis/BAC/oxime solution, also containing a small portion of the fluorescein methacrylamide monomer (compound characterization in Figures S10–S12, Supporting Information), enabled the incorporation of the oxime gel onto silk, as well as visualization of the gel layer (fluorescein isothiocyanate (FITC) filter: Exc. 490 nm/Em. 525 nm) due to random polymerization of the fluorescent monomer (silk has no autofluorescence at that excitation wavelength, Figure S13, Supporting Information). The size of the fabric pores was shown to significantly decrease upon gel impregnation and water equilibration (Figure 5g,h). Upon malaoxon addition, a significant number of pores fully closed, blocking bulk convection, owing to the gel mechanical actuation and triggering in response to the agent (Figure 5i; Figure S14, Supporting Information). Though the technology seems effective in fabric pore closing in many areas, the whole piece of fabric was not fully sealed. It is possible that uneven gel coating led to hydrogel-rich areas where the decontamination of the agent causes full pore sealing (Figure S14, Supporting Information), and hydrogel-poor areas where pores decrease significantly in size, but still remain open (Figure S15, Supporting Information). Work toward full fabric sealing is currently being pursued.

Oxime gel coated silk fabric in bulk contact with malaoxon displayed similar actuation as the fabric samples exposed to

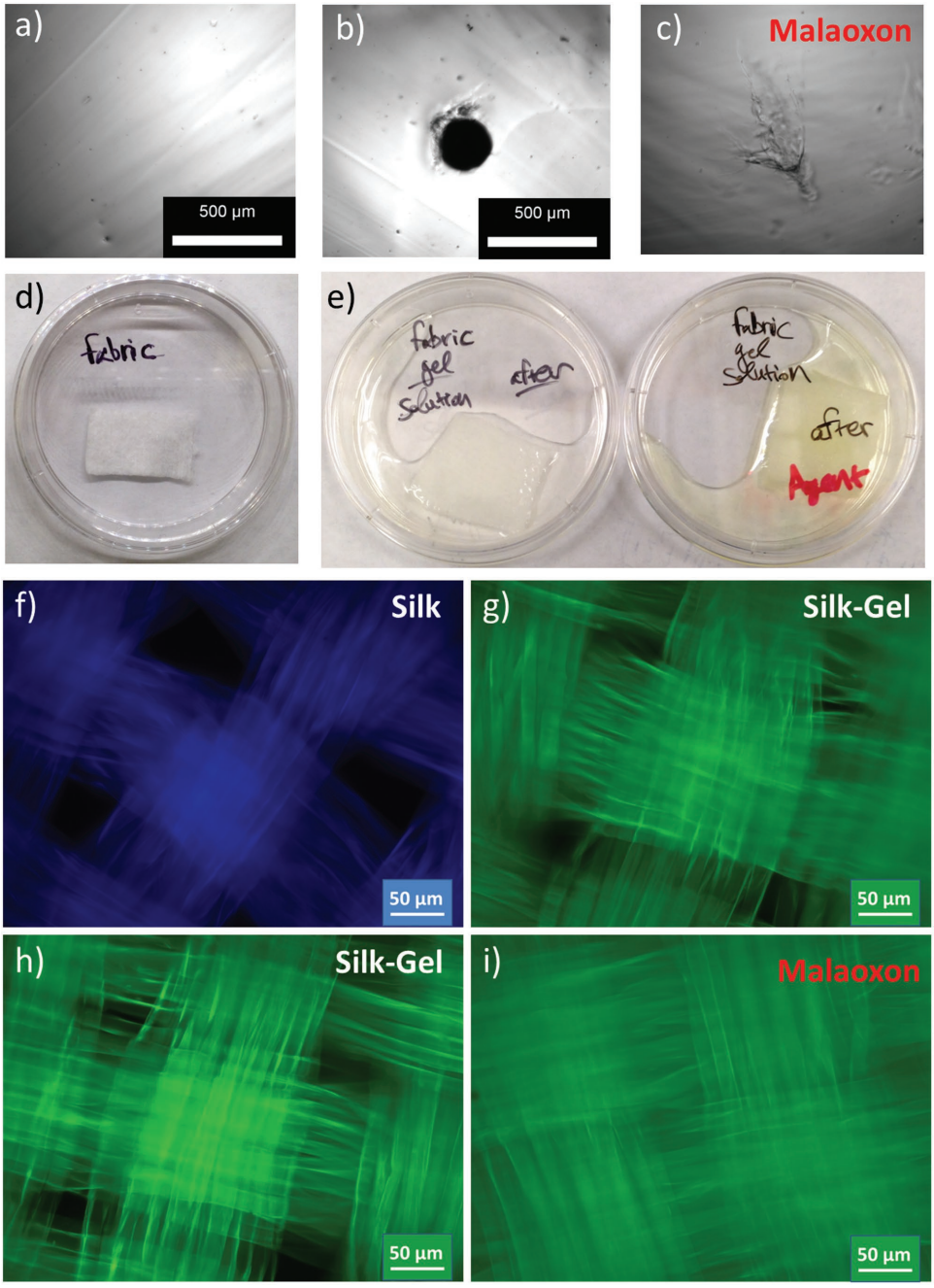

Figure 5. Optical microscope images of equilibrated oxime gels a) before and b) after perforation using microneedle arrays, as well as c) after swelling in the presence of malaoxon. The black holes represent punctured gels that swell and fill the voids. d) Nonwoven fabric and e) equilibrated oxime gel-coated fabric before and after the addition of malaoxon. The colorimetric assay (Ellman's reagent) of oxime-protected fabric confirms the reactivity of the fabric in response to the toxic agent. f) Autofluorescence of hydrated neat silk at 358 nm excitation. g,h) Silk polymerized with 30 wt% AAM/Bis/BAC/oxime/fluorescein methacrylamide after water equilibration at 490 nm excitation. i) Pore closing of silk/30 wt% oxime gel after addition of malaoxon. Images were collected at 600 ms exposure apart from neat silk which was collected at 1200 ms exposure.

malaoxon in solution. This test is designed to mimic direct contact of the gel with an aerosol which would deposit a layer of organophosphate on the outer surface of a garment. Lower concentrations of malaoxon (1 mg cm^{-2}) were used to coat coverslips, allowing for physical contact between the toxin and the fabric (**Figure 6**a) and possibly better replication of a realistic exposure route. Similar to the solution exposed fabric, fabrics in bulk contact had variable extents of pore closure after 22 h of exposure, with some areas showing full pore closure while other pores were qualitatively smaller but not fully closed (Figure 6b–d), likely due to variation in contact between the fabric and coverslip.

While the above tests match lethal dose, 50% (LD_{50}) values for malaoxon, they fail to replicate the common testing conditions.

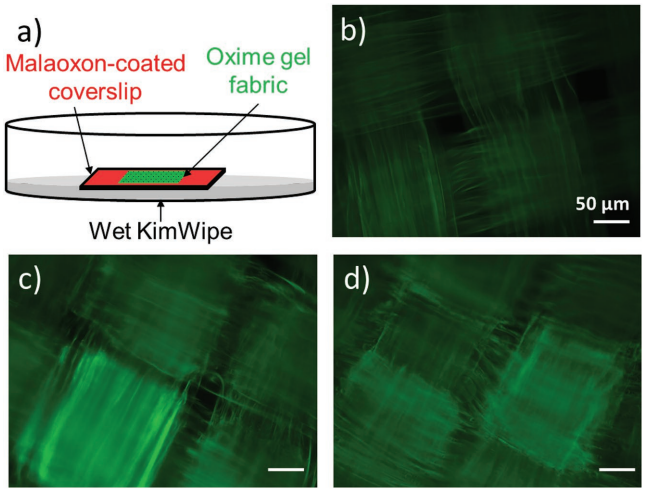

Figure 6. a) Schematic of bulk contact assay with oxime gel fabrics. Hydrated oxime gel-coated silk fabric b) before malaoxon (1 mg cm^{-2} on coverslip) addition. Malaoxon contact resulted in areas with c) fully closed pores and others with d) significantly decreased pore sizes. Images were collected at 600 ms exposure.

2 mL of the highest malaoxon concentration used (73.0×10^{-3} M) corresponds to a malaoxon mass of ≈46 mg. This is lower than the reported LD_{50} value for malaoxon oral exposure in male rats (≈55 mg for a male rat of 350 g mean weight),[57] and even lower than LD_{50} values reported for larger animals.[58] Though the reported LD_{50} value for the nerve agent VX (lowest lethal dose (LDLo) = 225 µg kg^{-1} for intravenous administration in human or 86 µg kg^{-1} LDLo after skin contact)[59] is much lower than malaoxon, the primary thiols that are liberated after reaction of VX with oximes are expected to react faster with the disulfide cross-linker than the liberating secondary thiols of malaoxon. For these reasons, both malaoxon and VX can be decontaminated via contact with these oxime gels. Typical material tests with toxic organophosphate compounds are performed in the range of 5–10 g m^{-2} (0.5–1 mg cm^{-2}). The 8 wt% oxime gels that were used in the gel swelling experiments were pipetted in round molds of 2.2 cm diameter, covering an area of 3.80 cm^2 ($S = \pi r^2$). The lowest malaoxon concentration that was used (18.3×10^{-3} M or 5.75 mg mL^{-1}) leads to ≈3 mg malaoxon cm^{-2}, which is 3–5 times higher than typical testing conditions. However, dosing of coupons at 1 mg cm^{-2} shows efficacy at doses within the normal range. Although the swelling response is not immediate, during the response organophosphate is actively being degraded. Changes in the thickness of the gel, as well as the ratio between oximes/Bis/BAC, could be tuned in order to accelerate response times at low dosages and determine the best formula for soldier protection. In particular, substantial increases in oxime concentration either attached to the polymer or simply blended with the gel could significantly improve response time by speeding degradation kinetics.

The use of hydrogels as a pore-closing layer requires that the gels remain hydrated throughout their use. In practice, this requires contact with a continuous source of water. While this may be provided in many ways, one possible approach may be to use gel-coated fabrics as a middle or inner layer in a protective garment, where perspiration from the wearer during use provides a flux of water to hydrate a thin gel barrier layer.

3. Conclusion

Oxime-containing hydrogels were prepared from inexpensive, commercially available materials, and were shown to react with the VX simulant malaoxon to produce a swelling response. The gels use a direct reaction of the organophosphate with oximes to decontaminate the hazardous compound. Coupling oxime-based decontamination and disulfide chemistry enabled generation of a system capable of decontamination and actuation in response to toxin exposure. The gel swelling actuated by toxin exposure was used to close pores and swell gel that has been coated on fibers. Incorporation of the synthesized acryl-EG_5-pyridine-4-aldoximes into poly(acrylamide) using N,N-*bis*(acryloyl cystamine) and free radical polymerization at room temperature enabled the formation of responsive gels that could be used as VX-sensors. Additionally, utilization of a second bridging molecule such as Bis enabled the selective response to be either complete dissolution or gel swelling, incorporating an additional sensing mechanism. Our strategy was used to coat fabric, leading to a response against malaoxon that closed pores in either a gel membrane or a fabric coating, acting as a second skin to shield against nerve agent simulants.

4. Experimental Section

Materials: Pyridine-4-aldoxime (98%) was purchased from Santa Cruz Biotechnology. Bromo-PEG_5-alcohol (96%) was purchased from Broadpharm. Pyridine-4-aldoxime, AAM, Bis, BAC, acryloyl chloride, pyridine-2-aldoxime methochloride, DTNB, 2-hydroxy-4′-(2-hydroxyethoxy)-2-methylpropiophenone (Irgacure 2959), N-(3-aminopropyl)methacrylamide hydrochloride, DTT, and malaoxon, were purchased from Sigma-Aldrich. Ammonium persulfate (APS) and N,N,N′,N′-tetramethylethylenediamine (TEMED) were purchased from VWR. NHS-fluorescein (5/6-carboxyfluorescein succinimidyl ester), mixed isomer, was purchased from Thermo Fisher Scientific Inc. Microneedle arrays were purchased from nanoBioSciences LLC.

Characterization of Chemical Structures: ^{1}H NMR spectroscopy (500 MHz) was performed using a Varian Inova 502 spectrometer. The spectra of the synthesized monomers were acquired in CD_3CN. Liquid chromatography-mass spectrometry (LC-MS) was performed using an Agilent 1260 Infinity Quaternary LC System, equipped with an Agilent 6130 MS spectrometer. The flow rate of the high performance liquid chromatography (HPLC) solvent (water/acetonitrile = 95/5 in volume) was 0.55 mL min^{-1}. Analysis was performed in the positive ionization mode. UV–vis spectra were collected on a Cary 50 UV–vis spectrophotometer with Peltier temperature controller using a quartz cuvette at concentrations reported below.

Synthesis of EG_5-pyridine-4-aldoxime (EG_5-oxime): Quaternization of pyridine-4-aldoxime was achieved by refluxing bromo-EG_5-alcohol (250 mg, 8.33×10^{-4} mol, 300 g mol^{-1}) with pyridine-4-aldoxime (305 mg, 25×10^{-4} mol, 122.05 g mol^{-1}, ×3 equiv.) in acetonitrile (10 mL) at 80 °C for 3 d. The product was then cooled down, and the solvent was removed under vacuum. Fresh acetonitrile was added, and the crude product was purified using a column with 3:1 dichloromethane/methanol (DCM/MeOH) as the mobile phase. The pure product was a yellow oil (yield 90%–95%) and was characterized by ^{1}H NMR and LC-MS (Figures S2–S4, Supporting Information). ^{1}H NMR (500 MHz, *CD3CN*) δ 8.94 (2H), 8.34 (1H), 8.23 (2H), 4.79 (2H), 3.99 (2H), 3.70-3.40 (16H); R_f = 0.26 (DCM/MeOH = 3:1); LC-MS *m/z* 343 [M-Br].

Synthesis of EG_5-pyridine-4-aldoxime Acrylate (Acryl-EG_5-oxime): EG_5-pyridine-4-aldoxime (113 mg, 0.33×10^{-3} mol, 343 g mol^{-1}) was dissolved in 4 mL acetonitrile, and acryloyl chloride (33 mg, 0.3 , 90.5 g mol^{-1}, ×1.1 equiv.) in 0.5 mL acetonitrile was added. Finally, triethylamine (37 mg, 0.36×10^{-3} mol, 101.19 g mol^{-1}, ×1.1 equiv.) in 0.5 mL acetonitrile was added dropwise at 0 °C and the reaction was left overnight. The crude product was then filtered, and the clear solution was concentrated under vacuum, leaving a yellow crystalline solid material. Purification was performed using a column with 5:1 DCM/MeOH as the mobile phase. The pure product was a yellow solid (yield 90%), and was characterized by ^{1}H NMR and LC-MS (Figures S5 and S6, Supporting Information). ^{1}H NMR (500 MHz, *CD3CN*) δ 8.94 (2H), 8.34 (1H), 8.23 (2H), 6.59 (1H, acryl), 6.32 (1H, acryl), 6.10 (1H, acryl), 4.79 (2H), 3.99 (2H), 3.70-3.40 (16H); R_f = 0.45 (DCM/MeOH = 5:1); LC-MS *m/z* 397 [M-Br].

Synthesis of N-(3-methacrylamidopropyl)fluorescein Amide (Fluorescein Methacrylamide): N-(3-Aminopropyl)methacrylamide hydrochloride (31 mg, 0.174×10^{-3} mol, 178.1 g mol^{-1}) and NHS-fluorescein (90.6 mg, 0.191×10^{-3} mol, 473 g mol^{-1}, ×1.1 equiv.) were dissolved in 1.5 mL dimethylformamide (DMF), and triethylamine (22.9 mg, 0.226×10^{-3} mol, 101.19 g mol^{-1}, ×1.3 equiv.) in 0.5 mL DMF was added dropwise, leading immediately to color change. The reaction was stirred overnight, and the product was precipitated in chloroform to remove excess triethylamine hydrochloride salts. The final product was dissolved in acetone and characterized by LC-MS (Figures S10–S12, Supporting Information). LC-MS *m/z* 501 [M+H]. Excitation/Emission 490/525 nm.

Formation of AAM/BAC/Oxime Hydrogels: 9 wt% AAM, 0.39 wt% BAC, 0.43 wt% acryl-EG_5-oxime (AAM/BAC/oxime) hydrogels were synthesized by free radical polymerization at room temperature. In all cases, the monomer molar ratios were AAM/BAC/oxime 115:1.4:1. Since the oximes react with malaoxon in a slow, rate-determining step, yielding thiolate ions, the number of the disulfide cross-linkers (that react with thiolates in a faster step) was engineered to be in excess relative to the oxime, so as to accelerate the response. Typically, AAM (180 mg, 2530 µmol) and BAC (8 mg, 31 µmol) were added, in a vial containing the appropriate amount of acryl-EG_5-oxime (8.8 mg, 22 µmol) and 1.91 mL of 25% ethanol solution was added. The monomers were heated for 5 min at 50 °C until complete dissolution, and then were cooled down at RT for 10 min. Next, a 10 wt% APS solution (94 µL, 41 µmol) was added to the reaction mixture, and the vial was vortexed to mix. The mixture was degassed by bubbling with nitrogen for 5 min. Subsequently, TEMED (45 µL, 300 µmol) was added under nitrogen flow so as to initiate the polymerization. The vial was sealed and vortexed for 10 s. Gel formation occurred at room temperature within 8–10 min. Vials were then left to polymerize for an additional 14 h. The gels were finally swollen in water for 3 d, in order to equilibrate, with water changed twice daily to remove any soluble fraction that eluted from the gel. As a control, 9 wt% AAM/BAC gels were prepared and swollen under the same conditions.

Formation of AAM/Bis/BAC/Oxime Hydrogels: 8 wt% AAM, 0.45 wt% Bis, 0.39 wt% BAC, 0.43 wt% acryl-EG_5-oxime (AAM/Bis/BAC/oxime) hydrogels were synthesized by free radical polymerization at room temperature, fixing the Bis/BAC molar ratio at 2:1 so that there are twice as many permanent cross-links as chemically labile cross-links. In all cases, the monomer molar ratios were AAM/Bis/BAC/oxime 101:2.8:1.4:1. Typically, AAM (160 mg, 2250 µmol), Bis (9.2 mg, 60 µmol), and BAC (8 mg, 31 µmol) were added in a vial containing the appropriate amount of acryl-oxime (8.8 mg, 22 µmol), and 1.91 mL of 25% ethanol solution was added. The monomers were heated for 5 min. at 50 °C until complete dissolution, and then were cooled down at RT for 10 min. Next, a 10 wt% APS solution (94 µL, 41 µmol) was added to the reaction mixture, and the vial was vortexed to mix. The mixture was degassed by bubbling with nitrogen for 5 min. Subsequently, TEMED (45 µL, 300 µmol) was added under nitrogen flow so as to initiate the polymerization. The vial was sealed and vortexed for 5 s. Before gelation but after the initiation of polymerization, the solution was pipetted into sealed molds of different shapes in order to obtain shaped gel structures. Gel formation occurred within 2–3 min. at room temperature. Vials were then left to polymerize for an additional 14 h. The gels were finally swollen in water for 3 d, in order to equilibrate, with water changed twice daily to remove any soluble polymer fraction that eluted from the gel. As a control, 8 wt% AAM/Bis/BAC gels were prepared and swollen under the same conditions.

Gel Erosion and Gel Swelling Studies: Freshly prepared malaoxon solutions were added (73.0×10^{-3}, 36.5×10^{-3}, and 18.3×10^{-3} M) to equilibrated AAM/BAC/oxime gels, and gel erosion studies were performed by measuring the weight of the remaining, cross-linked gel, after removing the liquid to another vial, and sequentially transferring it back. Control experiments were performed with water and DTT (73×10^{-3} M). For gel swelling experiments, different malaoxon solutions were added (73.0×10^{-3}, 36.5×10^{-3} M, 18.3×10^{-3} M) to equilibrated AAM/Bis/BAC/oxime gels. Chemical compounds that are found in sweat (such as urea, lactate, NaCl, ammonia, *p*-cresol) as well as other reactive chemicals (KOH, formic acid) were tested for gel swelling at the highest concentration (73×10^{-3} M) in order to show selectivity. Control swelling experiments were also performed with DTT at 73.0×10^{-3} M. In the case of AAM/Bis/BAC, the cloudy gels turned transparent upon swelling.

Integration of Oxime Hydrogels onto Fabric: Silk was selected as a model fabric for gel impregnation due to its relatively smooth, uniform fibers, making visualization of the gel layer clearer. Silk was plasma treated in air for two minutes, and was then immersed in acetonitrile containing acryloyl chloride, in order to modify the fabric with acrylate groups. The reaction was stirred overnight, and the fabric rinsed multiple times with water and finally dried at RT. A piece of modified fabric was then dipped in a coating bath containing 0.5 mL of a 30 wt% AAM/Bis/BAC/oxime solution (at 101:2.8:1.4:1 molar ratios) that also contained 10 µL of a 2×10^{-6} M fluorescein methacrylamide as well as Irgacure 2959 (2 wt%), and placed vertically in a scintillation vial. The vial was degassed by bubbling with nitrogen for 5 min, sealed, and UV-treated for 15 min, leading to polymerization. The oxime-gel containing fabric was left to polymerize for an additional 14 h, and was then immersed in water for three days, with two water changes per day. Gel swelling was performed as described for the gels using 73.0×10^{-3} M malaoxon solutions.

Bulk Malaoxon Contact with Oxime Hydrogel Fabrics: Silk fabrics integrated with oxime hydrogels were made as described before. Samples were imaged at 490 nm with an exposure time of 600 ms. Malaoxon solution (diluted in dichloromethane) was coated onto coverslips and evaporated to achieve a concentration of 1 mg cm^{-2}. Some areas of the coverslip contained viscous solutions of malaoxon and were uniformly spread over the surface of the coverslip as best as possible prior to applicaiton of the silk sample. Hydrated oxime-integrated silk samples were placed onto the malaoxon-coated coverslips and sealed in a petri dish (60 mm diameter) containing a wetted KimWipe to keep the fabric hydrated. The fabric remained in contact with the malaoxon coverslip for 22 h at which point the samples were reimaged to visualize gel swelling.

Model Fitting: In order to estimate rate constants of the reaction between pyridine-aldoxime and malaoxon in the presence of the thiol scavenger, DTNB, kinetics were modeled as two sequential pseudo-first order reactions (Figure S1, Supporting Information). By using high oxime/malaoxon as well as high DTNB/malaoxon molar ratios, the concentration of the produced benzyl-thiolate ions of TNB^2 (monitored at 412 nm), was modeled by the following equation

$$[TNB^{2-}] = [Mal.]_0 \times \left(1 + \frac{k_1 e^{-k_2 t} - k_2 e^{-k_1 t}}{k_2 - k_1}\right) \quad (1)$$

where $[TNB^{2-}]$ is the concentration of the produced benzyl-thiolate ions measured by UV–vis (ε = 14140 M^{-1} cm^{-1} in phosphate buffer, pH = 8), $[Mal.]_0$ is the initial concentration of malaoxon, k_1 is the apparent rate constant of the reaction between the oxime and malaoxon ($k_1 = k_{ox.} \times [oxime]_0$), and k_2 is the apparent rate constant of the reaction between the liberated thiolate ions and DTNB ($k_2 = k_{s.} \times [DNTB]_0$).

Gel erosion kinetics were fit to the empirical Korsmeyer–Peppas model[60] based on the following equation

$$[M_t / M_\infty] = kt^n \quad (2)$$

where M_t/M_∞, is the fractional gel eroded, t is the release time, k is a kinetic constant characteristic of the polymer system, and n is an exponent which characterizes the mechanism of release. For Fickian diffusion $n = 0.5$, anomalous diffusion is described by $0.5 < n < 1$, while for zero-order release behavior (time-independent release) $n = 1$. In the case of cylindrical gels (our case) or samples with particles size distribution, erosion profiles with values of $n < 0.5$ have been reported.[61–63]

Following gel swelling studies in solution, the effective cross-linked chains per g of polymer, U_e, were calculated, using the method of Bray and Merrill,[64,65] which is described by the following equation

$$U_e = \frac{\ln(1-U_{p,s}) + U_{p,s} + \chi U_{p,s}^2}{-\overline{V_s}\rho_p U_{p,r}\left[\left(\frac{U_{p,s}}{U_{p,r}}\right)^{1/3} - \frac{2}{F}\left(\frac{U_{p,s}}{U_{p,r}}\right)\right]} \quad (3)$$

$$U_{p,r} = \frac{1}{\frac{\rho_p}{\rho_s}(q_f - 1) + 1} \quad (4)$$

$$U_{p,s} = \frac{1}{\frac{\rho_p}{\rho_s}(q_s - 1) + 1} \quad (5)$$

where $U_{p,r}$ and $U_{p,s}$ are the volume fractions of gel upon formation (relaxed state) and after swelling (values after water equilibration and after malaoxon addition were calculated), χ is the Flory–Huggins interaction parameter for polyacrylamide (PAAM) and water at 25 °C (0.48), $\overline{V_s}$ is the molar volume of the solvent (≈18.0 mL mol^{-1}), ρ_p is the bulk density of PAAM at 25 °C (1.11 g mL^{-1}), F is the junction functionality ($F = 4$ for this system), ρ_s is the density of the solvent at 25 °C (≈1.00 g mL^{-1}), q_f is the weight ratio after gel preparation ($q_f = W_{rel}/W_{dry}$), and q_s represents weight swelling ratio after either water equilibration for 3 d ($q_w = W_{water}/W_{dry}$) or after malaoxon addition ($q_{mal} = W_{mal}/W_{dry}$). W_{rel} is the relaxed gel weight, W_{dry} is the dry gel weight, W_{water} is the swollen gel weight, and W_{mal} is the gel weight after incubation with malaoxon.

To characterize the nature of the oxime hydrogel networks that contain both permanent (Bis) and labile cross-links (BAC), the number of effective cross-links (U_e) was normalized to the number of cross-links (forming Bis and BAC molecules) in each gel at the time of cross-linking, to give a new quantity U_e* defined as

$$U_e^* = \frac{U_e}{U_{e_{max}}} = \frac{U_e}{\left(\frac{f_{Bis} + f_{BAC}}{f}\right) \times \left(\frac{1}{\overline{MW}}\right)} \quad (6)$$

$$\overline{MW} = \frac{x_{Bis}MW_{Bis} + x_{BAC}MW_{BAC}}{x_{Bis} + x_{BAC}} = 0.666MW_{Bis} + 0.333MW_{BAC} \quad (7)$$

where f is the total mass fraction of monomers in solution at the time of cross-linking; f_{Bis} and f_{BAC} are the mass fractions of Bis and BAC at the time of polymerization; X_{Bis} and X_{BAC} are the molar fractions of Bis and BAC, respectively (Bis/BAC = 2:1); and MW_{Bis} and $MW_{BAC}$are the molecular weights of Bis and BAC. In a perfect network with no entanglements, U_e* should be equal to 1 since all of the cross-linker chains participate in the network.

Supporting Information

Supporting Information is available from the Wiley Online Library or from the author.

Acknowledgements

This work was supported by the Defense Threat Reduction Agency under contract W911NF-07-D-0004. The authors acknowledge the MIT Department of Chemistry Instrumentation Facility for the NMR instrumentation.

Received: June 6, 2016
Revised: September 7, 2016
Published online: December 27, 2016

[1] D. Purves, G. J. Augustine, D. Fitzpatrick, W. C. Hall, A.-S. LaMantia, J. O. McNamara, L. E. White, *In Neuroscience*, 4th ed., Sinauer Associates, Sunderland, MA, USA **2008**.
[2] S. A. Bernhard, L. E. Orgel, *Science* **1959**, *130*, 625.
[3] J. Jarv, *Bioorg. Chem.* **1984**, *12*, 259.
[4] H. C. Froede, I. B. Wilson, *J. Biol. Chem.* **1984**, *259*, 11010.
[5] I. M. Kovach, *J. Enzyme Inhib.* **1988**, *2*, 199.
[6] M. Qian, I. M. Kovach, *FEBS Lett.* **1993**, *336*, 263.
[7] D. M. Quinn, *Chem. Rev.* **1987**, *87*, 955.
[8] C. B Millard, G. Kryger, A. Ordentlich, H. M. Greenblatt, M. Harel, M. L. Raves, Y. Segall, D. Barak, A. Shafferman, I. Silman, J. L. Sussman, *Biochemistry* **1999**, *38*, 7032.
[9] S.-B. Hong, F. M. Raushel, *Biochemistry* **1996**, *35*, 10904.
[10] H. Shim, F. M. Raushel, *Biochemistry* **2000**, *39*, 77357.
[11] S. D. Aubert, Y. Li, F. M. Raushel, *Biochemistry* **2004**, *43*, 5707.
[12] S. R. Samples, F. M. Raushel, V. J. DeRose, *Biochemistry* **2007**, *46*, 3435.
[13] A. J. Russell, J. A. Berberich, G. E. Drevon, R. R. Koepsel, *Annu. Rev. Biomed. Eng.* **2003**, *5*, 1.
[14] A. N. Bigley, C. Xu, T. J. Henderson, S. P. Harvey, F. M. Raushel, *J. Am. Chem. Soc.* **2013**, *135*, 10426.
[15] I. Cherny, P. Greisen Jr., Y. Ashani, S. D. Khare, G. Oberdorfer, L. Haim, D. Baker, D. S. Tawfik, *ACS Chem. Biol.* **2013**, *8*, 2394.
[16] C. H. Lei, Y. S. Shin, J. Liu, E. J. Ackerman, *J. Am. Chem. Soc.* **2002**, *124*, 11242.
[17] P. B. Dennis, A. Y. Walker, M. B. Dickerson, D. L. Kaplan, R. R. Naik, *Biomacromolecules* **2012**, *13*, 2037.
[18] P. L. Havens, H. F. Rase, *Ind. Eng. Chem. Res.* **1993**, *32*, 2254.
[19] K. E. LeJeune, A. J. Mesiano, S. B. Bower, J. K. Grimsley, J. R. Wild, A. J. Russell, *Biotechnol. Bioeng.* **1997**, *54*, 105.
[20] K. E. LeJeune, J. R. Wild, A. J. Russell, *Nature* **1998**, *395*, 27.
[21] K. E. LeJeune, J. R. Wild, A. J. Russell, *Biotechnol. Bioeng.* **1999**, *62*, 659.
[22] Y. Lee, I. Stanish, V. Rastogi, T.-C. Cheng, A. Singh, *Langmuir* **2003**, *19*, 1330.
[23] B. N. Novikov, J. K. Grimsley, R. J. Kern, J. R. Wild, M. E. Wales, *J. Controlled Release* **2010**, *146*, 318.
[24] W. Wei, J. Du, J. Li, M. Yan, Q. Zhu, X. Jin, X. Zhu, Z. Hu, Y. Tang, Y. Lu, *Adv. Mater.* **2013**, *25*, 2212.
[25] M. Kim, M. Gkikas, A. Huang, J. W. Kang, N. Suthiwangcharoen, R. Nagarajan, B. D. Olsen, *Chem. Commun.* **2014**, *50*, 5345.
[26] T. J. Dale, J. Rebek Jr., *J. Am. Chem. Soc.* **2006**, *128*, 4500.
[27] S. Bencic-Nagale, T. Sternfeld, D. R. Walt, *J. Am. Chem. Soc.* **2006**, *128*, 5041.
[28] J. G. Weis, T. M. Swager, *ACS Macro Lett.* **2015**, *4*, 138.
[29] F. Hobbiger, P. W. Sadler, *Br. J. Pharmacol.* **1959**, *14*, 192.
[30] D. Kuhnen-Clausen, I. Hagedorn, G. Gross, H. Bayer, F. Hucho, *Arch. Toxicol.* **1988**, *54*, 171.
[31] G. Amitai, H. Murata, J. D. Andersen, R. R. Koepsel, A. J. Russell, *Biomaterials* **2010**, *31*, 4417.
[32] J. Lovrić, S. Berend, A. Lucić-Vrdoljak, B. Radić, M. Katalinić, Z. Kovarik, D. Želježić, N. Kopjar, S. Rast, M. Mesić, *Acta Biochim. Pol.* **2011**, *58*, 193.
[33] J. Jin, V. Nguyen, W. Gu, X. Lu, B. J. Elliot, D. L. Gin, *Chem. Mater.* **2005**, *17*, 224.

[34] H. Grosfeld, D. Barak, A. Ordentlich, B. Velan, A. Shafferman, *Mol. Pharmacol.* **1996**, *50*, 639.
[35] J. Kassa, *J. Toxicol. Clin. Toxicol.* **2002**, *40*, 803.
[36] F. Worek, G. Reiter, P. Eyer, L. Szinicz, *Arch. Toxicol.* **2002**, *76*, 523.
[37] K. Kuca, J. Bielavský, J. Cabal, J. Kassa, *Bioorg. Med. Chem. Lett.* **2003**, *13*, 3545.
[38] P. Eyer, *Toxicol. Rev.* **2003**, *22*, 165.
[39] F. Worek, H. Thiermann, L. Szinicz, P. Eyer, *Biochem. Pharmacol.* **2004**, *68*, 2237.
[40] F. Worek, L. Szinicz, P. Eyer, H. Thiermann, *Toxicol. Appl. Pharmacol.* **2005**, *209*, 193.
[41] K. Kuca, D. Juna, K. Musilek, *Mini-Rev. Med. Chem.* **2006**, *6*, 269.
[42] B. Antonijevic, M. P. Stojiljkovic, *Clin. Med. Res.* **2007**, *5*, 71.
[43] F. Worek, P. Eyer, N. Aurbek, L. Szinicz, H. Thiermann, *Toxicol. Appl. Pharmacol.* **2007**, *219*, 226.
[44] M. Jokanović, M. Prostran, *Curr. Med. Chem.* **2009**, *16*, 2177.
[45] N. Peppas, J. Z. Hilt, A. Khademhosseini, R. Langer, *Adv. Mater.* **2006**, *18*, 1345.
[46] M. Kim, S. Tang, B. D. Olsen, *J. Polym. Sci. Part B* **2013**, *51*, 587.
[47] M. Gkikas, R. K. Avery, B. D. Olsen, *Biomacromolecules* **2016**, *17*, 399.
[48] T. Miyata, N. Asami, T. Uragami, *Nature* **1999**, *399*, 766.
[49] M. Bajomo, J. H. G. Steinke, A. Bismark, *J. Phys. Chem. B* **2007**, *11*, 8655.
[50] G. Sicillia, C. Grainger-Boultby, N. Francini, J. P. Magnusson, A. O. Saeed, F. Fernández-Trillo, C. Alexander, *Biomater. Sci.* **2014**, *2*, 203.
[51] P. Wang, Y. Zhang, L. Cheng, W. Liu, *Macromol. Chem. Phys.* **2015**, *216*, 164.
[52] M. H. Lee, Z. Yang, C. W. Lim, Y. H. Lee, S. Dongbang, C. Kang, J. S. Kim, *Chem. Rev.* **2013**, *113*, 5071.
[53] X. Zhang, S. Malhotra, M. Molina, R. Haag, *Chem. Rev.* **2015**, *44*, 1948.
[54] G. L. Ellman, *Arch. Biochem. Biophys.* **1959**, *82*, 70.
[55] J. C. Gaulding, M. H. Smith, J. S. Hyatt, A. Fernandez-Nieves, L. A. Lyon, *Macromolecules* **2012**, *45*, 39.
[56] I. Georgakoudi, I. Tsai, C. Greiner, C. Wong, J. Defelice, D. Kaplan, *Opt. Express* **2007**, *15*, 1043.
[57] W. C. Dauterman, A. R. Main, *Toxicol. Appl. Pharmacol.* **1966**, *9*, 408.
[58] National Institute for Occupational Safety and Health (NIOSH), Malathion: Immediately Dangerous to Life and Health.
[59] U.S. Department of the Army, Army Environmental Center, *J. Toxicol. Environ. Health Part A* **2000**, *59*, 439.
[60] R. W. Korsmeyer, R. Gurny, E. Doelker, P. Buri, N. A. Peppas, *Int. J. Pharm.* **1983**, *15*, 25.
[61] N. A. Peppas, *Int. J. Pharm.* **1983**, *15*, 25.
[62] P. L. Ritger, N. A. Peppas, *J. Controlled Release* **1987**, *5*, 23.
[63] P. Costa, J. M. Sousa Lobo, *Eur. J. Pharm. Sci.* **2001**, *13*, 123.
[64] J. C. Bray, E. W. J. Merrill, *Appl. Polym. Sci.* **1973**, *17*, 3779.
[65] J. A. Beamish, J. Zhu, K. Kottke-Marchant, R. E. Marchant, *J. Biomed. Mater. Res. A* **2010**, *92*, 441.